



**HAL**  
open science

## Dielectric and electrical properties of radiation-cured epoxy

Bertrand Vissouvanadin, G. Teyssedre, Séverine Le Roy, Christian Laurent,  
G. Ranoux, Xavier Coqueret

► **To cite this version:**

Bertrand Vissouvanadin, G. Teyssedre, Séverine Le Roy, Christian Laurent, G. Ranoux, et al.. Dielectric and electrical properties of radiation-cured epoxy. *IEEE Transactions on Dielectrics and Electrical Insulation*, 2015, 22 (2), pp.1142-1150. 10.1109/TDEI.2015.7076816 . hal-02431691

**HAL Id: hal-02431691**

**<https://hal.univ-reims.fr/hal-02431691>**

Submitted on 3 Oct 2022

**HAL** is a multi-disciplinary open access archive for the deposit and dissemination of scientific research documents, whether they are published or not. The documents may come from teaching and research institutions in France or abroad, or from public or private research centers.

L'archive ouverte pluridisciplinaire **HAL**, est destinée au dépôt et à la diffusion de documents scientifiques de niveau recherche, publiés ou non, émanant des établissements d'enseignement et de recherche français ou étrangers, des laboratoires publics ou privés.

# Dielectric and Electrical Properties of Radiation-Cured Epoxy

B. Vissouvanadin\*, G. Teyssedre\*, S. Le Roy\*, C. Laurent\*,  
G. Ranoux\*\* and X. Coqueret\*\*

\*LAPLACE, University of Toulouse, 118 route de Narbonne, F-31062 Toulouse Cedex 9, France

\*\* ICMR, Université de Reims Champagne-Ardenne, CNRS UMR 7312, F-51687 Reims Cedex 2, France

To cite: B. Vissouvanadin, G. Teyssedre, S. Le Roy, C. Laurent, G. Ranoux, X. Coqueret, "Dielectric and electrical properties of radiation-cured epoxy", IEEE Trans. Dielectr. Electr. Insul. 22, 1142-1150, 2015. DOI: 10.1109/TDEI.2015.7076816

**Abstract**— Dielectric and electrical properties of radiation-cured epoxy are investigated in various conditions of electric field and temperature for different initiator content. The impact of the onium salt initiator is particularly considered due to the formation of ionic species that can impact the electrical properties. Dielectric spectroscopy performed in the temperature range  $-80^{\circ}\text{C}$  to  $+200^{\circ}\text{C}$  and the frequency range  $10^{-1}$  to  $10^6$  Hz shows that  $\beta$ -relaxation of the cured resin and relaxation due to ionic species are dominating the dielectric behavior at low and high temperature respectively. Water absorbed in the resin increases the dielectric losses and conduction current. Ionic and electronic charge carriers are seen to dominate the electrical behavior at low and high field respectively. No clear trend has been observed as regard the effect of initiator concentration on the dielectric and electrical properties of radiation-cured epoxy.

**Index Terms** – Radiation curing, epoxy, dielectric and electrical properties

## 1 INTRODUCTION

Radiation curing shows multiple advantages when compared to the classical thermal curing process. A main advantage is that it does not require heating as for thermal process and can be achieved at ambient temperature. Another advantage is that no by-product is generated unlike for thermal curing process which mostly affects material properties. In addition, curing under ionizing radiation enables a fast manufacturing [1]. Up to now, radiation curing is mainly used as an alternative to UV technology for curing inks, paints, coatings and adhesives by cross-linking polymerization. It is also used for curing of carbon fiber-reinforced composites for aeronautic and spatial applications. Applications to processing of high voltage electrical insulation are very seldom. However, radiation curing can be interesting if the electrical properties of the material can be tailored.

For the cationic polymerization of epoxies, an initiator is required. Diaryliodonium salts (DAIS) are mostly used since they are easily reduced by free radicals produced by e-beam irradiation of the epoxide resin substrate as well as by direct reduction [2]. Consequently, a high conversion ratio can be obtained with a low concentration of DAIS [2]. A post curing

is performed after vitrification to complete the polymerization process as the polymer matrix may still contain active sites. For conversion ratio up to 90%, the post curing treatment induces a decrease in the material glass transition temperature ( $T_g$ ). This decrease of  $T_g$  has been attributed to some relaxation of weakly-bonded ion pair clusters trapped inside the matrix during vitrification. Their thermal relaxation induces a decrease of the network cross-link density and therefore the network  $T_g$  [3]. Further, a network with a higher degree of heterogeneity seems to be formed when using low concentration of initiator [4]. This means that a sufficiently high initiator concentration is required to achieve an homogeneous network. However, inclusion of ion pairs in the material network from the initiator is also likely to have an impact on the material electrical properties as they could participate in the conduction mechanism. In this contribution, we report on the dielectric and electrical properties of radiation-cured epoxies as a function of the cationic initiator concentration and sample conditioning.

## 2 EXPERIMENTAL

### 2.1 SAMPLES

Epoxy samples have been elaborated using the base model resin Diglycidyl Ether of Bisphenol A (DGEBA with  $n \approx 0.05$ ). The onium salt initiator for electron beam irradiation curing was cumyltolyliodonium tetrakis (pentafluorophenyl borate) ( $\text{Ar}_2\text{I}^+$ ,  $\text{B}(\text{C}_6\text{F}_5)_4^-$ ) named DAIS in the following. The chemical structure of DAIS is shown in Figure 1.

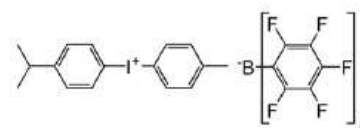


Figure 1: Chemical structure of DAIS (taken from [3]).

Electron Beam (EB) radiation is produced by a pulsed accelerator (10 MeV, 20 kW, time-averaged of 15 kGy/s). A total dose of 100 kGy has been deposited on plaque samples of 1 mm thickness for the curing process. Samples containing various concentrations of DAIS (from 0.125 wt to 2% wt) have been elaborated. A post curing thermal treatment at

190°C for 90 min was achieved prior to dielectric characterization. Because of the pseudo living character of cationic polymerization and the various periods of time between sample elaboration and electrical measurements, we intended to bring the samples (1 or 2 mm-thick plates) to a controlled and stabilized level of conversion. Hence this post-baking procedure was applied to all samples.

Materials T<sub>g</sub> were estimated by Differential Mechanical Analysis (DMA) to 176, 174, 168 and 155°C respectively for samples cured with 0.125, 0.5, 1 and 2% DAIS at 1Hz [3].

## 2.2 CHARACTERIZATION TECHNIQUES

Three different characterization techniques which are dielectric spectroscopy, current-voltage and space charge were used to investigate electrical and dielectric properties of various epoxies formulations. For all tests, gold electrodes were beforehand deposited onto both faces of each sample by sputtering. For dielectric spectroscopy, frequency-domain dielectric measurements were performed in the range 10<sup>-1</sup> to 10<sup>7</sup> Hz during a heating run from -80 up to +200°C using a *Novocontrol Alpha-a* high resolution dielectric analyzer. Measurements have been carried out on unconditioned (kept in ambient conditions for several days) and conditioned samples (treated at 50°C for 2 days). The conditioning was achieved for bringing the samples into a similar reference state with respect to moisture sorption. DC current measurements were carried out using a *Keithley 617* electrometer on samples with 5 cm diameter circular electrode at 3 different temperatures for DC fields between 2 and 25 kV/mm. To avoid possible memory effects due to sample pre-stressing, a new sample was used for each test at a given temperature. Space charge measurements have been realized using the Pulsed Electro-Acoustic Method (PEA) [5] at 25°C and for field ranging from 5 to 20 kV/mm. Each polarization step lasts for 1 h and is followed by a depolarization step of the same duration. Space charge profiles were acquired both in polarization and depolarization. The polarization time of 1h was chosen so that the discharge current is substantially lower than the charging current. In all the test conditions presented in this work, the depolarization current after 1h did not exceed 10% of the charging current. In this way, the transient current processes due to polarization effects can be neglected, and steady state conduction is supposed to be approached – even though there may subsist some transient contributions due to space charge effects.

## 3 DIELECTRIC PROPERTIES

### 3.1 FROM -80°C TO +50°C

For temperatures below 50°C, the permittivity is about 4 and is relatively stable in the investigated frequency range. The evolution of the dielectric losses between -80 and 50°C is shown in Figure 2 for various frequencies. A relaxation peak is observed for each frequency and moves toward higher temperature as the frequency increases. This corresponds to the  $\beta$ -relaxation of the cured resin which may be attributed to

the crankshaft rotation of hydroxyether groups [6]. Such a relaxation obeys the Arrhenius law. From the data of Figure 2 the activation energy and the pre-exponential factor have been estimated to be about 0.75 eV and 1.7x10<sup>18</sup> Hz respectively, which are typical values for such a process. Furthermore, increasing initiator content does not affect either the pre-exponential factor or the activation energy, which strengthens the interpretation in terms of molecular motion.

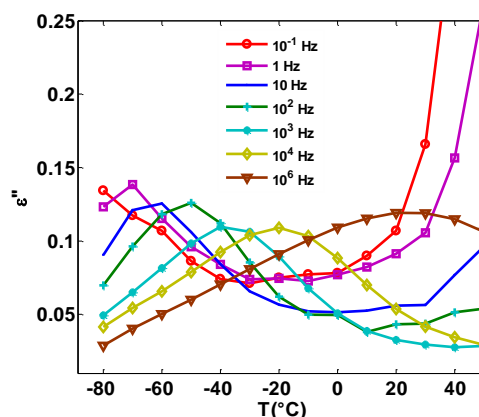
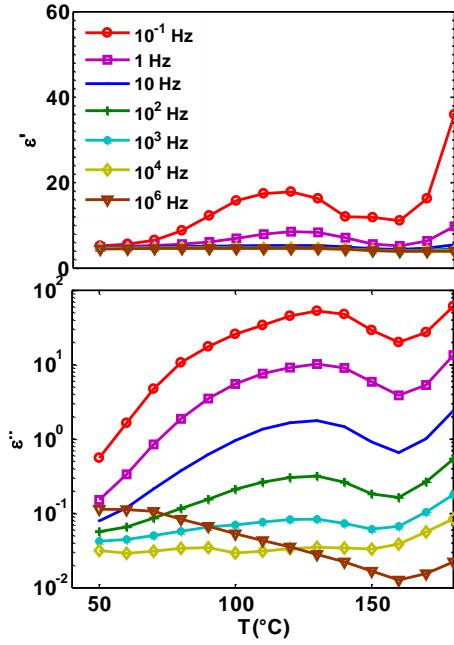


Figure 2: Dielectric losses vs. temperature in the range -80°C to +50°C at different frequencies for a cured sample with 1% DAIS.

### 3.2 FROM +50°C TO +150°C

Dielectric permittivity and losses as a function of temperature are represented in Figure 3 for frequencies between 10<sup>-1</sup> and 10<sup>+6</sup> Hz. In this temperature range both permittivity and losses increase, especially at low frequencies, and reach a maximum at around 120°C ( $\epsilon'' = 40$  at 0.1 Hz). A concomitant increase of permittivity and losses at low frequency is encountered when ionic species are involved in the conduction mechanism. As electrodes are generally blocking for ionic species, ionic conduction gives rise to heterocharges formation adjacent to the electrodes under sufficiently low frequency. Such distribution of charge behaves as a macroscopic dipole and produces an increase in the permittivity at low frequency: the later reaches a value  $\epsilon'' = 20$  at 0.1 Hz and 120°C in Figure 3.

The evolution of the loss tangent ( $\tan \delta$ ) vs. frequency is shown in Figure 4 at different temperatures for various initiator contents. For all the samples, we note an increase of the loss tangent with a decreasing frequency typical of Low Frequency Dispersion (LFD) phenomena. All samples exhibit roughly a value of  $\tan \delta$  higher that 0.2 at 0.1 Hz. Furthermore all samples show a relaxation phenomenon occurring at frequency below 10 Hz. Such relaxation, labeled  $\rho$  in Figure 4, cannot be attributed to a dipolar relaxation as it is associated with a huge variation regarding both permittivity and losses for temperatures higher than 80°C in the case of 1% of DAIS (see Figure 3). Such behavior is attributed to space charge relaxation due to ionic space charge accumulated at the electrodes and forming a macroscopic dipole. An expression of the complex permittivity has been established by Coelho [7] in the case of macroscopic space-charge polarization assuming



**Figure 3:** Dielectric permittivity and losses vs. temperature in the range +50 to +180°C at different frequencies for a cured sample with 1% DAIS (untreated).

blocking electrodes:

$$\varepsilon^* = \varepsilon_\infty \frac{1 + i\omega\tau}{i\omega\tau + \frac{\tanh Y}{Y}} \quad (1)$$

where  $\omega$  and  $\tau$  are the radial frequency and the relaxation time respectively,  $\varepsilon_\infty$  the dielectric constant at high frequency.  $Y$  is related to the Debye length  $L_D$  (assigned to the space charge thickness) and the sample thickness  $d$  as follows:

$$Y = \frac{d}{2L_D} \sqrt{1 + i\omega\tau} = \kappa \sqrt{1 + i\omega\tau} \quad (2)$$

The Debye length depends on the carrier density  $n_0$  such as:

$$L_D = \frac{1}{e} \sqrt{\frac{\varepsilon_\infty \cdot k_B T}{n_0}} \quad (3)$$

where  $e$  and  $k_B$  are respectively the elementary charge and the Boltzmann's constant and  $T$  the temperature.

For low value of Debye length compared to the sample thickness, namely a high value of  $\kappa = d/2L_D$ , it can be proven that the loss tangent versus frequency reaches a maximum at the coordinates [8]:

$$(f_c, \tan(\delta)_{\max}) = \left( \frac{1}{2\pi\sqrt{\kappa}\tau}, \sqrt{\kappa}/2 \right) \quad (4)$$

By locating the coordinates of a local maximum in the  $\tan(\delta)$  vs. frequency curves (see  $\rho$  on Figure 4), one can derive the corresponding Debye length (thereby the carrier concentration) and the space charge relaxation time  $\tau$  using relation (3), for each temperature and each DAIS content. It is worth mentioning that at low frequency, several relaxation processes related to different relaxation time and/or Debye length may occur. Low magnitude relaxations (assigned to low

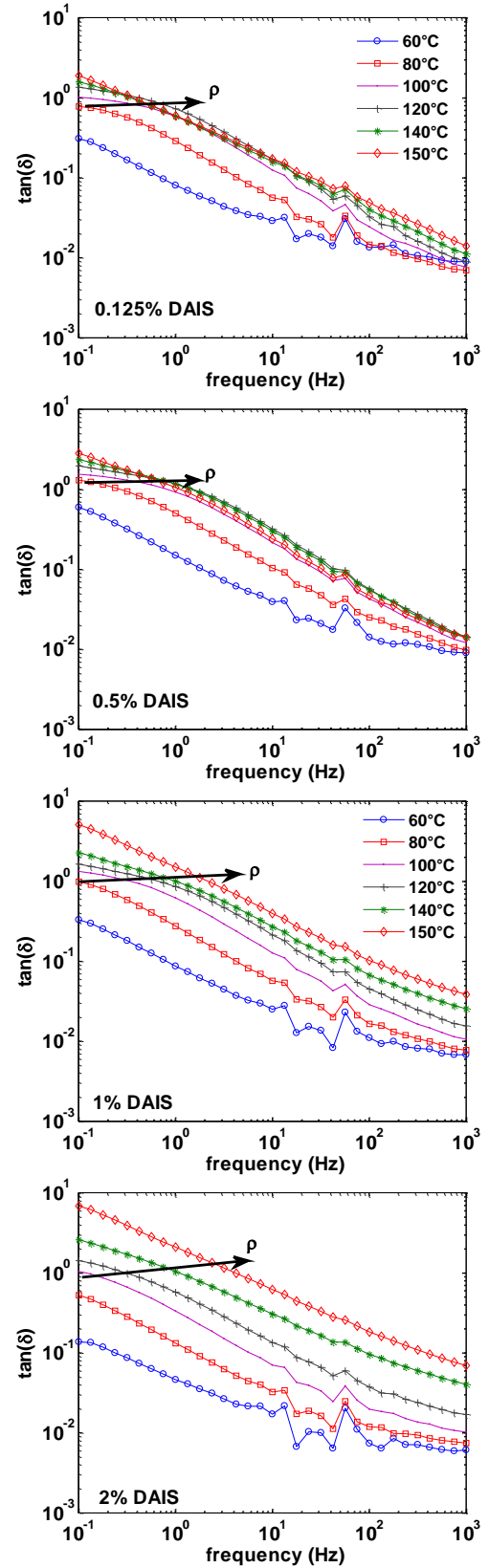


**Figure 4:**  $\tan(\delta)$  vs. frequency in the range of temperatures between 60 and 150°C for different initiator content (untreated).

carrier density according to (3)) may be overwhelmed by higher magnitude relaxations. Therefore, the uncertainty made on locating the loss tangent at its maximum will directly affect the accuracy of the carrier density and mobility estimates.

As the conductivity ( $\sigma$ ) is related to the carrier relaxation time as follows,

$$\tau = \frac{\epsilon_{\infty}}{\sigma} \quad (5)$$

the conductivity can be derived from the critical frequency and the related value of loss tangent, cf. equation (4):

$$\sigma = 4\pi f_c \epsilon_{\infty} \tan(\delta)_{\max} \quad (6)$$

Knowing the carrier concentration and the conductivity, the carrier mobility can be calculated, following:

$$\sigma = e n_0 \mu \quad (7)$$

From (6), the higher the critical frequency and the value of the corresponding loss tangent are, the higher is the conductivity. Data from Figure 4 reveal that the critical frequency increases with temperatures for all samples. Furthermore, in the studied range of temperature, the shift in frequency is increasing with the initiator content. For a constant value of  $\tan(\delta) = 1$ , the frequency changes from 0.1 (at 100°C) to 0.3 Hz (at 150°C) for 0.125 %wt DAIS containing sample while for the sample cured with 2% DAIS the frequency reaches 4.2 Hz (at 150°C) for the same value of  $\tan(\delta)$ . Since the material's Tg decreases with the initiator concentration, a higher shift in frequency, for formulations with lower Tg, is presumably related to an enhancement in the carriers mobility due to an increase in the free volume which facilitates ions displacement within the network.

Conversely, the values of  $\tan(\delta)_{\max}$  seem to remain rather stable taking values between 1 and 2 for all samples in the range of temperatures from 60°C to 150°C. We deduce from (3) and (4) that the value of  $\tan(\delta)_{\max}$  is proportional to  $(n_0/T)^{1/4}$  so that an increase by a factor 2 in respect to  $\tan(\delta)_{\max}$ , in the range of temperatures between 60 and 150°C, corresponds to an increase by a factor of about 20 in the carrier density indicating the possibility that carriers are thermally generated.

Computed values of charge density, mobility and conductivity are shown in Table 1 for various initiator contents from 80°C to 100°C. In this range of temperatures, values of  $\tan(\delta)_{\max}$  are rather constant so that the carrier density does not evolve considerably with temperature while the mobility seems to be thermally activated. Mobilities are rather high, taking values in the range from  $10^{-6}$  to  $10^{-5}$  m<sup>2</sup>/V/s. No clear trend has been found for the conductivity variation with respect to the initiator content.

### 3.3 FROM +160°C TO +200°C

For temperatures above 180°C and at high frequency, the real part of the permittivity drops to an unrealistic value that is probably due to a crushing of the electrode coating as the sample is in a rubbery state at these temperatures. This phenomenon leads to a decrease in the electrodes surface.

Thus, for high temperature both the real and the imaginary parts are inaccurate and may not be treated individually as they depend upon the sample geometry. However, their ratio - namely the loss tangent- is not affected by the geometry change. This issue has been subsequently resolved by using a larger set-up contact electrode.

**Table 1:** Carrier density, mobility and conductivity values computed from the Coelho model between 80 and 100°C for (untreated) epoxy samples cured with various initiator contents.

| DAIS % | Conduction parameters       | T°C                 |                     |                     |
|--------|-----------------------------|---------------------|---------------------|---------------------|
|        |                             | 80                  | 90                  | 100                 |
| --     | --                          | 80                  | 90                  | 100                 |
| 0.125  | $n_0$ (m <sup>-3</sup> )    | $10^{14}$           | $10^{14}$           | $10^{14}$           |
|        | $\mu$ (m <sup>2</sup> /V/s) | $3 \cdot 10^{-6}$   | $6 \cdot 10^{-6}$   | $12 \cdot 10^{-6}$  |
|        | $\sigma$ (S/m)              | $5 \cdot 10^{-11}$  | $10 \cdot 10^{-11}$ | $20 \cdot 10^{-11}$ |
| 0.5    | $n_0$ (m <sup>-3</sup> )    | $4 \cdot 10^{14}$   | $4 \cdot 10^{14}$   | $5 \cdot 10^{14}$   |
|        | $\mu$ (m <sup>2</sup> /V/s) | $2 \cdot 10^{-6}$   | $3 \cdot 10^{-6}$   | $5 \cdot 10^{-6}$   |
|        | $\sigma$ (S/m)              | $13 \cdot 10^{-11}$ | $20 \cdot 10^{-11}$ | $40 \cdot 10^{-11}$ |
| 1      | $n_0$ (m <sup>-3</sup> )    | $3 \cdot 10^{14}$   | $3 \cdot 10^{14}$   | $3 \cdot 10^{14}$   |
|        | $\mu$ (m <sup>2</sup> /V/s) | $10^{-6}$           | $1.4 \cdot 10^{-6}$ | $3 \cdot 10^{-6}$   |
|        | $\sigma$ (S/m)              | $5 \cdot 10^{-11}$  | $7 \cdot 10^{-11}$  | $14 \cdot 10^{-11}$ |
| 2      | $n_0$ (m <sup>-3</sup> )    | $3 \cdot 10^{13}$   | $5 \cdot 10^{13}$   | $6 \cdot 10^{13}$   |
|        | $\mu$ (m <sup>2</sup> /V/s) | $5 \cdot 10^{-6}$   | $5 \cdot 10^{-6}$   | $9 \cdot 10^{-6}$   |
|        | $\sigma$ (S/m)              | $2 \cdot 10^{-11}$  | $4 \cdot 10^{-11}$  | $9 \cdot 10^{-11}$  |

Tan  $\delta$  versus frequency is shown in Figure 5 for different initiator concentrations and at different temperatures. Samples with initiator content lower than 0.5%, exhibit one relaxation whilst samples cured with higher initiator content exhibit two relaxations. The two processes,  $\rho$  and  $\rho^*$  are materialized by arrows, in the continuity of data presented in Figure 4. The relaxation  $\rho$  in the case of 0.5% DAIS is suspected to be shaded or mixed with the relaxation  $\rho^*$ .

As previously mentioned, relaxation peaks give information about the nature of carrier distribution or the trap depth involved in the conduction mechanism. The evidence of two relaxation phenomena in the case of epoxy with 1 and 2% DAIS - epoxy may correspond to two kinds of carrier having different mobilities.

This would be the case when ions and electronic carriers or anions and cations for example were involved in the transport mechanism. The result would be the same if only one kind of carrier were involved with two levels of trap, being deep and shallow. As previously mentioned, a high value of  $\tan(\delta)_{\max}$  corresponds to a high concentration of carrier. Figure 5 reveals that the maximum of the loss tangent does not change considerably with temperature. This means that carrier concentration does not change substantially with temperature. Furthermore since the density of carriers is related to the magnitude of relaxation, the density of carriers involved in  $\rho^*$  relaxation is higher than in  $\rho$  relaxation. For 1% DAIS, carrier concentration has been estimated to be about  $2 \cdot 10^{20}$  m<sup>-3</sup> and  $10^{16}$  m<sup>-3</sup> respectively for  $\rho^*$  and  $\rho$  relaxations. For 2% DAIS, concentration of  $2 \cdot 10^{19}$  m<sup>-3</sup> for  $\rho^*$  and values between  $10^{16}$  and  $2 \cdot 10^{16}$  m<sup>-3</sup> for  $\rho$  have been found. For relaxation  $\rho^*$ , cured sample with 0.125% DAIS shows a carrier concentration



between  $2 \cdot 10^{19}$  and  $5 \cdot 10^{19} \text{ m}^{-3}$ . These values show that there is no real dependence of the carrier concentration with the

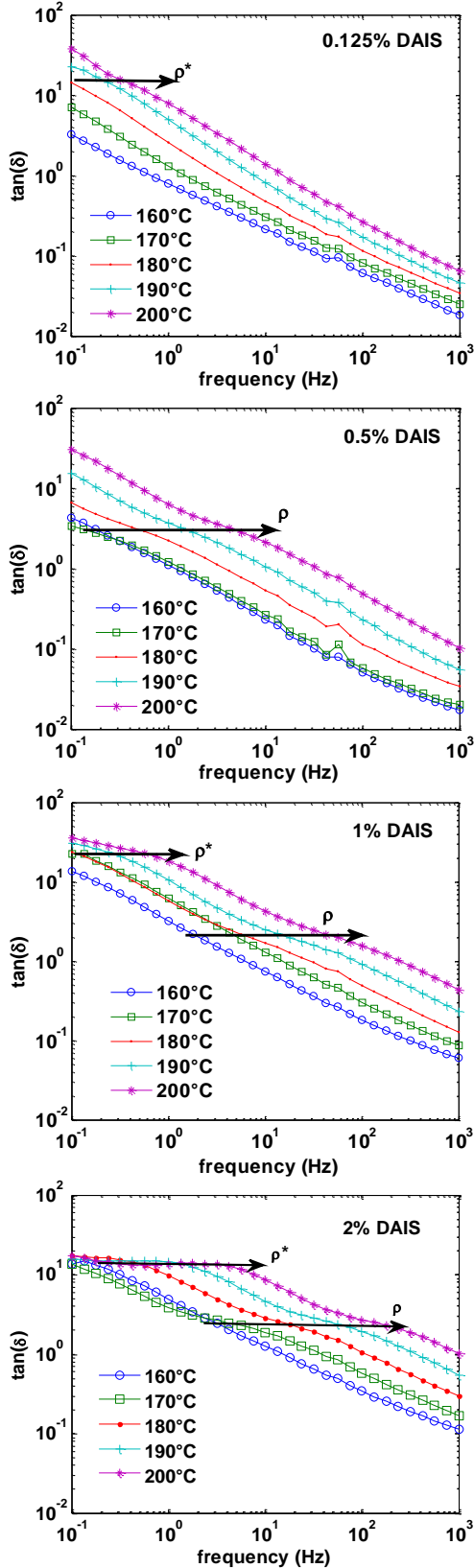


Figure 5 : Tan ( $\delta$ ) vs. frequency at various temperatures for different initiator contents (untreated).

initiator content. The latter is not the only ion source available in the material. Indeed, the water uptake may have an impact on the carrier density. In the next section we investigate the impact of drying on dielectric losses.

Unlike the carrier density, the critical frequency  $f_c$  moves to higher value as temperature increases due to the thermally activated nature of the relaxation time and carrier mobility. For a given relaxation, as the carrier concentration remains stable with temperature, the mobility would increase with the critical frequency according to the relations (4), (5) and (7). Following this scheme, relaxation  $\rho^*$  would be related to relatively slow carriers with mobility varying between  $5 \cdot 10^{-11}$  and  $2 \cdot 10^{-7} \text{ m}^2/\text{V}\cdot\text{s}$ . Relaxation  $\rho$  would be produced by fast carriers for which mobility is about 5 orders of magnitude higher than for  $\rho^*$  relaxation.

Figure 6 represents Arrhenius plots of carriers mobility (computed at 180, 190 and 200°C) related to  $\rho^*$  and  $\rho$  relaxations for 1% and 2% DAIS. Slow carriers exhibit activation energies of 1 and 1.6 eV whereas fast carriers show activation energies of 1.2 and 1.6 eV.

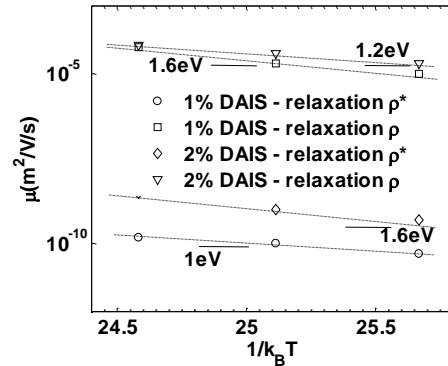
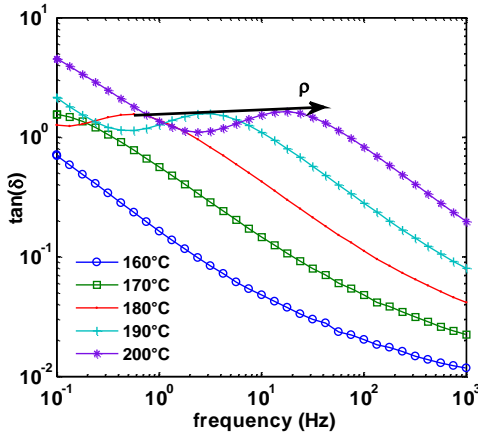


Figure 6 : Arrhenius plot of charge mobilities computed from the Coelho model for 1 and 2% DAIS (temperature being 180, 190 and 200°C).

### 3.4 EFFECT OF CONDITIONING ON PERMITTIVITY AND LOSSES

Results presented in the previous section were obtained on samples stored in ambient environment for a long time before measurements. Part of the dielectric response might be related to absorbed water. The effect of absorbed water on the properties of epoxy resin has been widely addressed in the literature and is known to induce a serious impact on both the mechanical and electrical properties of the material [9], [10], [11].

Dielectric spectroscopy measurements have been carried out on samples conditioned at 50°C for 2 days. This conditioning reduces the water content in the materials. Dielectric permittivity and losses are represented in Figure 8 for a cured sample with 1% DAIS. In the range of 50 to 150°C, the real part of permittivity keeps almost the same value for all frequencies unlike for untreated sample for which the permittivity goes through a maximum around 120°C (Figure 3). In addition losses are reduced by a factor 40 at



**Figure 7:** Tan ( $\delta$ ) versus frequency for various temperatures showing the  $\rho$  relaxation for epoxy cured with 1% DAIS (dried).

least compared to untreated samples. Conditioning enables to reduce both low frequencies losses and permittivity between 50 and 150°C so that the drying process is likely to reduce the ionic conduction within the material. However, above 160°C, the sample still exhibits steep increase in both permittivity and losses at low frequency which is the signature of Low Frequency Dispersion Phenomenon described in the previous section.

Figure 7 represents the loss tangent vs. frequency of treated sample of cured epoxy with 1% DAIS. Unlike for untreated samples, only one relaxation is observed. Given the magnitude of  $\tan \delta$ , the relaxation type is related to the  $\rho$  relaxation already observed for untreated samples. Different parameters related to the conduction mechanism (computed from Coelho model) are shown in Table 2. Carrier density is estimated to around  $3 \cdot 10^{15} \text{ m}^{-3}$  and is relatively stable with temperature.

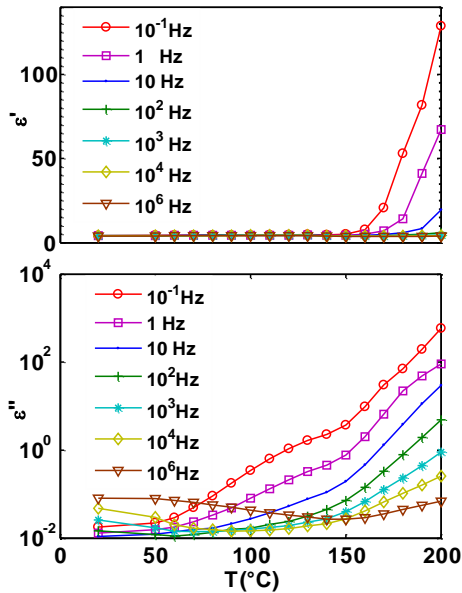


**Figure 8:** Permittivity and losses v.s temperature at various frequencies (from  $10^{-1}$  to  $10^6$ Hz) for a cured sample with 1% DAIS (dried).

The corresponding Debye length is about  $50 \mu\text{m}$ . Charge mobility and therefore the conductivity are thermally activated as evidenced by the shift of the max of  $\tan \delta$  to higher frequency when temperature increases. Activation energy of the conductivity is estimated to about 3.4 eV which is about twice that obtained in the case of untreated sample for the same process. Furthermore, the  $\rho^*$  relaxation due to low mobility carriers is likely suppressed by the effect of conditioning. This suggests that water contained in untreated sample may promote low mobility carriers thus contribute to the increase of the material conductivity.

**Table 2:** Conduction parameters for dried sample of epoxy cured with 1% DAIS at temperature between 180 and 200°C.

| Conduction parameters          | T°C                  |                     |                      |
|--------------------------------|----------------------|---------------------|----------------------|
|                                | 180                  | 190                 | 200                  |
| $n_0 \text{ (m}^{-3}\text{)}$  | $3 \cdot 10^{15}$    | $3 \cdot 10^{15}$   | $4 \cdot 10^{15}$    |
| $\mu \text{ (m}^2\text{/V/s)}$ | $7 \cdot 10^{-7}$    | $4 \cdot 10^{-6}$   | $2 \cdot 10^{-5}$    |
| $\sigma \text{ (S/m)}$         | $3.4 \cdot 10^{-10}$ | $19 \cdot 10^{-10}$ | $130 \cdot 10^{-10}$ |

## 4 ELECTRICAL PROPERTIES

### 4.1 CURRENT-VOLTAGE CHARACTERISTIC

The current-voltage characteristics at temperatures of 25, 40 and 53°C for EB-cured epoxy with 1% DAIS are presented in Figure 9. The current values, taken after 1 hour of polarization, are considered as quasi-steady state current. For fields lower than 10 kV/mm and temperatures of 25 and 40°C, current vs. electric field characteristics follow a quasi-linear behavior as a function of field. At 55°C, a deviation from Ohm's law is observed, which is an indication that conduction may be controlled by charge injection at this temperature. Such a sub-linear behavior may be the result of diffusion-limited Schottky emission which holds in certain conditions especially when the mobility of electrons is low and therefore the carrier thermal energy density predominate over the electrostatic field energy density [12].

A hyperbolic sine law, derived from hopping and ionic conduction has been used to fit the experimental data [13]:

$$I_C = A \cdot \exp\left(\frac{-E_A}{kT}\right) \cdot \sinh\left(\frac{\lambda \cdot E}{2kT}\right) \quad (8)$$

where A is a constant,  $E_A$  is the activation energy (in eV), k is the Boltzman's constant ( $8.62 \cdot 10^{-5} \text{ eV/K}$ ),  $\lambda$  is the hopping distance. The fitting lines are plotted on Figure 9 for current-field characteristics of cured epoxy with 1% DAIS at different temperatures. A good correlation between experimental and theoretical data is obtained. A hopping distance of about 5 nm and 4 nm has been derived from samples cured with respectively 1% DAIS and 0.25% DAIS. Hence, the density of hopping sites would be slightly decreasing with the increase in DAIS content. The reason may be that a lower content of initiator leads to a material with a higher level of heterogeneity and therefore a higher concentration of defects compared to the material cured with higher initiator content.

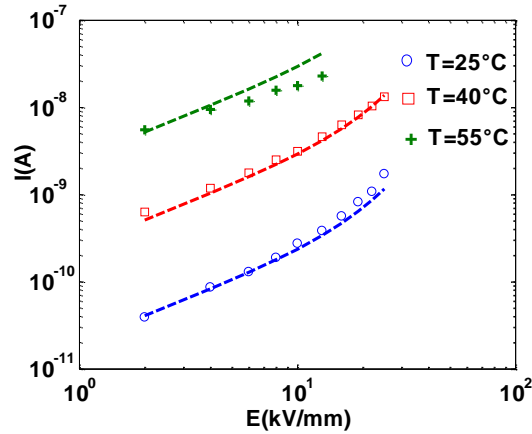


**Figure 9:** Current-Voltage characteristics at different temperatures radiation cured epoxy with 1% DAIS (untreated). Lines represent the fit obtained from the conduction model.

For untreated epoxy cured with 1% DAIS, the activation energy of the conductivity for fields  $\leq 10$  kV/mm is estimated to be about 1.6 eV. For samples cured with 0.25% of DAIS, conductivity at 25°C is the same order of magnitude and lies around  $2.10^{-14}$  (S/m) whereas the activation energy of the conductivity is approximately 1 eV. This difference can be explained by the difference in the glass transition temperature which has been estimated from DMA measurement (performed at 1Hz) to be 184°C and 173°C for 0.25% and 1% DAIS, respectively. The material with higher glass transition temperature is expectedly less sensible to the temperature increase as regard to the conductivity.

### 4.2 EFFECT OF CONDITIONING ON CONDUCTIVITY

Table 3 compares the values of conductivity of treated and untreated epoxy samples cured with 1% DAIS derived from current-voltage measurement carried out at 2 kV/mm. We notice for untreated sample a rather good agreement between measured dc conductivity and the values derived from dielectric spectroscopy measurements. Indeed, conductivity of unconditioned sample, derived from the value of charging current after 1 hour of polarization under 2 kV is  $1.4 \times 10^{-12}$  S/m at 55°C and is estimated to be about  $8.10^{-11}$  S/m at 80°C assuming a constant activation energy of 1.6 eV between 25 and 80°C. The value obtained using Coelho model was  $5.10^{-11}$  S/m for the same condition (Table 1).

Conductivity of conditioned samples is lower by a factor of at least 20 when compared to unconditioned samples. As already pointed out for dielectric losses, conductivity of EB-cured epoxy is likely to be sensitive to the sample moisture.

**Table 3:** Conductivity in S/m measured at 2 kV/mm at various temperatures for treated and untreated samples of epoxy cured with 1% DAIS.

| Conductivity (S/m) | Temperature          |                      |                      |
|--------------------|----------------------|----------------------|----------------------|
|                    | 25°C                 | 40°C                 | 55°C                 |
| 1% DAIS            |                      |                      |                      |
| Treated            | $6.0 \cdot 10^{-16}$ | $1.0 \cdot 10^{-15}$ | $6.0 \cdot 10^{-14}$ |
| Untreated          | $1.0 \cdot 10^{-14}$ | $1.6 \cdot 10^{-13}$ | $1.4 \cdot 10^{-12}$ |

### 4.3 SPACE CHARGE

Space charge profiles and corresponding protocol of voltage application on unconditioned sample with 1% DAIS is shown in Figure 10. The pattern reveals charge injection at both electrodes during volt-on at 25°C for fields from 5 to 20 kV/mm and charge densities increase with the applied electrical stress. Charge injection apparently dominates from the lowest applied field of 5 kV/mm. Another striking point is the detection of positive charges adjacent to the former cathode (lower electrode) that seem to appear progressively during depolarization. These positive charges are distinguished from image charges as their peak position slightly moves towards the bulk of the insulation in the course of depolarization. It can be thought that as negative charges depletion is faster than that of positive charges in the vicinity of the former cathode, hence positive charges become predominant after a while during volt-off. For reconciling this behavior with the contribution of ionic species in the low field behavior of the material found in impedance spectroscopy, it is suggested the existence of two types of charged species coming from injection and from dissociation. Injected charges from the electrodes will take the lead on charge transport because they dominate the charge distribution in volt-on. Salt dissociation will give rise to the ionic species that contribute to the formation of heterocharges near the electrodes. Ionic species are likely to dominate the electrical behavior at low field explaining the dielectric behavior (measurements were made under 1 V). At higher fields, electronic injected charges dominate and control the transport behavior.

Two remarks can be made as regards electronic injection and transport. First the efficiency of the injection process is evidenced from the lowest field of 5 kV/mm. This seems to indicate a low injection barrier at the electrode/epoxy contact

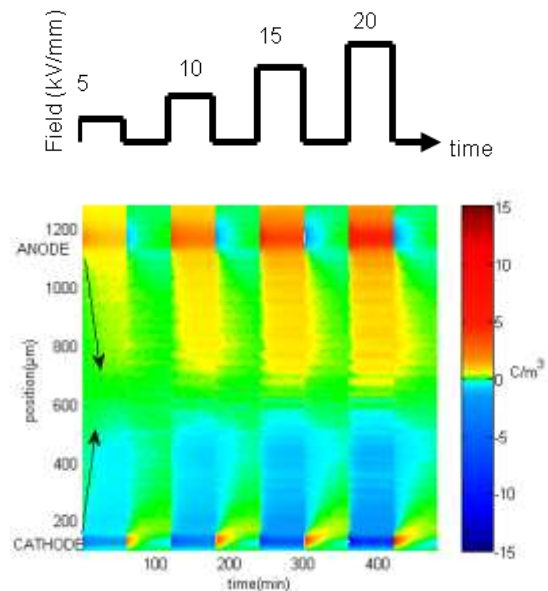


**Figure 10 :** Top: Applied poling field, Bottom: Space charge plot for untreated epoxy sample cured with 1% DAIS for field from 5 to 20 kV/mm and T=25°C.



for both anode and cathode. In particular, transfer between the Fermi level and the electronic levels assisting transport could be envisaged owing to the complex chemical formulation of the material. Second, estimation of the charge mobilities, made considering the propagation front of positive and negative charge carriers during the first step in field, gives a value of about  $10^{-10}$  m<sup>2</sup>/V.s. Extrapolation of mobility at 25°C of fast carriers (corresponding to the  $\rho$  relaxation) from dielectric measurement, considering an activation energy of 1.6 eV, leads to a value of the same order of magnitude as obtained from space charge suggesting that electronic charges (injected from electrodes due to the field enhancement induced by accumulated ionic charges) is likely to be responsible of the  $\rho$  relaxation previously observed.

## 5 CONCLUSION

Dielectric and electrical properties of radiation-cured epoxy have been investigated in various conditions of electric field and temperature. The dielectric behavior below 50°C is dominated by the  $\beta$ -relaxation of the cured resin attributed to individual motion of hydroxyether groups. At higher temperature, space charge relaxations involving two kinds of carriers being slow and fast have been highlighted. The Coelho model was used to derive their respective density and mobility. The slow carriers are thought to be promoted by water absorbed during sample storage and tend to increase considerably the dc conductivity and therefore the dielectric losses of epoxy samples. Space charge measurements have revealed two components of the current at room temperature being ionic and electronic. This seems to indicate that ions from dissociated salt are highly mobile but the ionic component is dominated by electronic transport at moderate applied field. No clear trend has been observed as regards to the effect of initiator content on the dielectric and electrical properties of radiation-cured epoxy. Conduction effect due to water absorption may be predominant over the effect of initiator content. However, lower initiator content seems to give rise to a higher density of traps which may be correlated to the higher level of heterogeneity of the material.

## ACKNOWLEDGMENT

The authors acknowledge the support of the French Agence Nationale de la Recherche (ANR), under grant ANR-MAPR09-443689 (project ICIP).

## REFERENCES

- [1] R.L. Clough, "High-energy radiation and polymers: A review of commercial processes and emerging applications", Nucl. Instr. and Meth. in Phys. Res. B, Vol. 185, pp. 8-33, 2001.
- [2] J.V. Crivello, T.C. Walton, and R. Malik, "Fabrication of Epoxy Matrix Composites by Electron Beam Induced Cationic Polymerization", Chem. Mater., Vol. 9, pp. 1273-1284, 1997.
- [3] G. Ranoux, M. Molinari, and X. Coqueret, "Thermo-mechanical properties and structural features of diglycidyl ether of BIS phenol a

cationically cured by electron beam radiation", Radiat. Phys. Chem., Vol. 81, pp. 1297-1302, 2012.

- [4] G. Ranoux, PhD thesis, University of Reims, to be published in 2014.
- [5] T. Maeno and K. Fukunaga, "High-resolution PEA Charge Distribution Measurement System", IEEE Trans. Dielectr. Electr. Insul., Vol. 3, pp. 754-757, 1996.
- [6] I.M. Kalogeras, M. Roussos, I. Christakis, A. Spanoudaki, D. Pietkiewicz, W. Brostow, and A. Vassilikou-Dova, "Dielectric properties of cured epoxy resin + poly(ethylene oxide) blends", J. Non-Cryst. Solids, Vol. 351, pp. 2728-2734, 2005.
- [7] R. Coelho, "Sur la relaxation d'une charge d'espace", Revue de Physique Appliquée, Vol. 18, pp. 137-146, 1983.
- [8] T.M.W.J. Bandara and B.E. Mellander, "Evaluation of Mobility, Diffusion Coefficient and Density of Charge Carriers in Ionic Liquids and Novel Electrolytes Based on a New Model for Dielectric Response", in Ionic Liquids: Theory, Properties, New Approaches, A. Kokorin (Ed.), InTech, 2001, pp. 383-406. ISBN 978-953-307-349-1.
- [9] E. Brun, P. Rain, G. Teissedre, C. Guillermin, and S. Rowe, "Hygrothermal aging of a filled epoxy resin", in Proc. 2007 IEEE International Conference on Solid Dielectrics, pp. 239-242, 2007.
- [10] C. Zou, M. Fu, J.C. Fothergill, and S.W. Rowe, "Influence of absorbed water on the dielectric properties and glass-transition temperature of silica-filled epoxy nanocomposites", in Proc. 2006 IEEE Conference on Electrical Insulation and Dielectric Phenomena, pp. 321-324, 2006.
- [11] K.I. Ivanova, R.A. Pethrick, and S. Affrossman, "Investigation of hydrothermal ageing of a filled rubber toughened epoxy resin using dynamic mechanical thermal analysis and dielectric spectroscopy", Polymer, Vol. 41, pp. 6787-6796, 2000.
- [12] P.R. Emtage and J.J. O'Dwyer, "Richardson-Schottky effect in insulators", Phys. Rev. Lett., Vol. 16, pp. 356-358, 1966.
- [13] S. Boggs, H. Dwight, J. Hjerrild, J.T. Holbol, and M. Henriksen, "Effect of Insulation Properties on the Field Grading of Solid Dielectric DC Cable", IEEE. Trans. Power. Delivery, Vol. 16, pp. 456-462, 2001.



(LAPLACE) in Toulouse.

**Bertrand Vissouvanadin** was born in Port-Bergé Madagascar, on September 1982. He received the Diploma in physics engineering from the National Institute of Applied Sciences, Toulouse, France, in 2007. He received the Ph.D. degree in electrical engineering of the university of Toulouse in 2011 for his work on synthetic materials for HVDC cables. As a post-doc, Dr. Vissouvanadin is currently involved in the study of electrical properties of radiation-cured epoxy at the Laboratory of Plasma and Energy Conversion



**Gilbert Teysedre** was born in May 1966 in Rodez, France. He received his Engineer degree in materials physics in 1989 at the National Institute for Applied Science (INSA) and graduated in solid state physics the same year. Then he joined the Solid State Physics Lab in Toulouse and obtained the Ph.D. degree in 1993 for work on transition phenomena and electro-active properties of fluorinated ferroelectric polymers. He entered the CNRS in 1995 and has been working since then at the Electrical Engineering Lab (now LAPLACE) in Toulouse. His research activities concern the development of luminescence techniques in insulating polymers with focus on chemical and physical structure, degradation phenomena, space charge and transport properties. He is currently Research Director at CNRS and is leading a team working on the reliability of dielectrics in electrical equipment.



**Séverine Le Roy** was born on 30 August 1977 in Belfort, France. She graduated in molecular and structural physical chemistry in 2001 at the Joseph Fourier University, Grenoble, France. Then she joined the Electrical Engineering Laboratory in Toulouse and obtained her Ph.D. degree in electrical engineering in 2004 from Paul Sabatier University. She entered the CNRS (National Centre of Scientific Research) in 2006. She is now dealing with modelling activities in relation with charge transport and ageing, for various domains of

applications like electrical engineering, spatial environment. She is also concerned in the relationship between experiments and simulations.



**Christian Laurent** (M'98-SM'07) was born in Limoges, France, in 1953. He studied solid state physics at the National Institute for Applied Sciences in Toulouse and received his Eng. degree in physics in 1976. He joined the Electrical Engineering Laboratory at Paul Sabatier University in 1977 to study electrical treeing and partial discharge phenomena, which were the topics of his Dr. Eng. degree (1979). He joined CNRS (National Centre for Scientific Research) in 1981 and got his Doc-ès Sc. Phys. in 1984. In 1985, he spent one year as a post-doctoral fellow with the IBM

“Almaden Research Center” where he studied plasma-polymerized thin films. Back in Toulouse he developed an approach to electrical ageing in polymeric materials based on luminescence analysis. He is now dealing with experimental and modeling activity relating to charge transport and ageing. He is currently Research Director at CNRS and Director of the Laboratory of Plasma and Energy Conversion -LAPLACE- in Toulouse.



**Guillaume Ranoux** was born on May 1979 in Mexico. He received his Master degree in formulation chemistry in 2004 at Lille 1 University, France. He has been working since 2008 at the Molecular Chemistry Institute of Reims (ICMR) where he prepared a PhD in macromolecular chemistry. His research activities deal with radiation induced cross-linking polymerization to elaborate composites with emphasis on polymerization kinetics, on structure-properties relations and on the microstructural aspects of radiation cured networks.



**Xavier Coqueret**, born in 1956, received his PhD in Organic Chemistry from the University of Reims in 1984. He joined at that time the Polymer Department at the University of Lille, as an associate scientist of the CNRS (Centre National de la Recherche Scientifique). He was appointed as Professor of Polymer Chemistry at the Ecole Nationale Supérieure de Chimie de Lille in 1991, and then moved to the University of Reims Champagne Ardenne in 2005. His activities include the electron beam-induced modification of polymers by cross-linking or by grafting, radiation-

initiated polymerization and materials derived from biomass. He teaches analytical chemistry, polymer chemistry and chemical valorization of bio-based materials. Since January 1<sup>st</sup> 2008, he is heading the Institute of Molecular Chemistry, a research Institute under contract with CNRS (UMR 7312).